

Short thesis for the degree of doctor of philosophy (PhD)

**Hydration mechanisms and drug delivery
applications of synthetic polymer aerogels**

by Krisztián Eduárd Moldován

Supervisor: Dr. József Kalmár



UNIVERSITY OF DEBRECEN

Doctoral School of Chemistry

Debrecen, 2023.

List of abbreviations

BNC	Budapest Neutron Centre
BSE	Backscattered Electron
CPMAS	Magic Angle Spinning
D_{obs}	Observed equilibrium diffusion coefficient
IUPAC	International Union of Pure and Applied Chemistry
MAS	Magic Angle Spinning
NMR	Nuclear Magnetic Resonance
PBS	Phosphate-buffered saline solution
R_g	Radius of gyration
SANS	Small Angle Neutron Scattering
SE	Secondary Electron
SEM	Scanning Electron Microscope

I. Introduction and aim

Aerogels are the world's lowest density solid materials (0.01-0.20 g/cm³) that have extremely high specific surface areas (200-1000 m²/g) and an open pore structures. Aerogels are characterized by an extremely low thermal conductivity (0.05–0.10 W/mK), which is why they are perhaps one of the most promising thermal insulator material families today. Aerogels have special physical and chemical properties among the solid materials, that is why they are studied in many research areas (space research, biomedical applications, construction and building industry).

Aerogels are produced in three main steps that affect their final structure. The most commonly used method for the preparation of their skeleton is the sol-gel method. In the first step, nano-sized sol particles are formed in the reactions of the starting reagents, which then turn into a gel network. The next step in the production of aerogels is solvent exchange, and the last step is drying with supercritical carbon dioxide.

The development of synthetic polymer aerogels was partly driven by the need for new, extremely low-density materials. Polyimide and polyamide aerogels are characterized by excellent mechanical properties and moisture stability.

Our research focuses on understanding the interaction of these porous materials with water, including the moisture content of the air. Hydration of aerogels is usually associated with microstructural changes, which also affect their mechanical properties. Due to their high specific surface area, aerogels are excellent carriers and delivery systems of drugs. Therefore we impregnated the aerogels with two drugs and then tested their release in different release media.

II. Methods

Solvated polymer gels were synthesized using the sol-gel process, and the last step in the preparation of aerogels was drying in supercritical CO₂. For this purpose, we used a device that does not require a liquid CO₂ pump. The system works with the original pressure of the submersible-tubed CO₂ cylinder and the pressure increase that occurs with the supercritical transition. The characterization of the aerogels was carried out using different structural analysis methods. We investigated the morphology of the aerogels with a scanning electron microscope (ThermoFisher Scientific Scios 2). To determine the specific surface area, pore size distribution and pore volume of the aerogels, nitrogen adsorption-desorption porosimetry measurements (Quantachrome Nova 2200e) were performed in accordance with IUPAC recommendations. The chemical structure of the produced aerogels was confirmed by Fourier transform infrared spectroscopy (Perkin Elmer Spectrum Two Spectrometer).

The size distribution of the aerogel particles dispersed in an aqueous medium was examined using an optical microscope with a 1.3 MP USB camera. The images were analyzed using the ImageJ software and the size of the particles was calculated from the image analysis. Zeta potential measurement was performed with MALVERN Zetasizer Nano ZS equipment with conventional instrument settings and automatically fine-tuned measurement parameters. The compressive strength of dry and partially hydrated aerogel monoliths was measured using an Instron 4302 instrument.

The small angle neutron scattering (SANS) measurements were carried out in cooperation with the researchers of the ELKH-EK Neutron Spectroscopy Laboratory. The measurements were carried out in the Budapest Neutron Centre (BNC), on the Yellow Submarine's pin-hole

type, equipped with a two-dimensional neutron detector. The solid-state NMR measurements were realized in collaboration with researchers from the Amadeo Avogadro University in Alessandria. Solid-state NMR spectra were recorded on a Bruker Avance III 500 spectrometer and an 11.75 Tesla magnet at operating frequencies of 500.13 and 125.77 MHz for ^1H and ^{13}C .

The NMR relaxometric measurements were performed with a Minispec Bruker mq20 relaxometer. The dry and partially hydrated aerogel samples were characterized by NMR cryoporometry and diffusometry at different water contents in a Bruker Avance II 360 MHz NMR device.

The impregnation of the aerogels with drugs were carried out in supercritical CO_2 , ensuring the appropriate contact time under static conditions. For the release studies, 2 media (pH = 1.0 hydrochloric acid and pH = 7.4 PBS) were used and the released amount of drug was monitored by UV-vis spectrophotometry (Hewlett-Packard 8453 photometer).

III. New scientific results

1. We proved that the gold sputtered on the surface of nanostructured aerogels affects the morphology seen in the images in the case of scanning electron microscopy (SEM).

1.1) We observed that sputtering even a thin, 5 nm gold layer (as recommended in the literature) results in the formation of artificial structural elements on the surfaces of many different types of aerogels, and the 16 nm thick layer significantly modifies the morphology of all the studied aerogels (Figure 1).

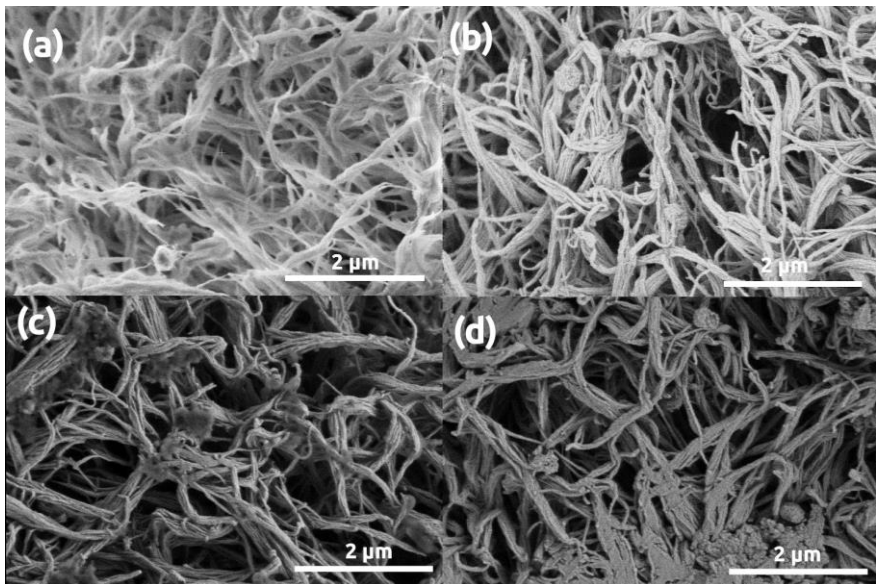


Figure 1. LVSEM images of polyamide aerogel samples. (a) Pristine, uncoated. (b–d) Sputter coated with 5 nm, 16 nm, 32 nm thick Au layers, respectively.

1.2) We have shown that the gold atoms condense on the nanostructured surfaces of the studied aerogel during sputtering and form mostly spherical Au nanoparticles (clusters) (Figure 2). The morphology of the sputtered gold structures could be visualized in the SEM instrument in high resolution in atomic number based contrast using a backscattered electron (BSE) detector.

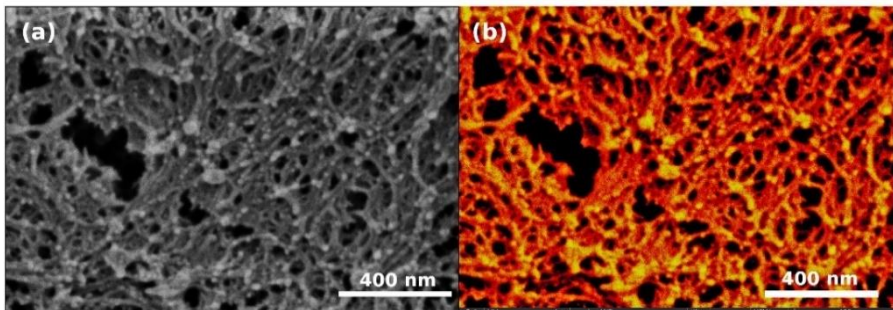


Figure 2. Images showing the combination of the as-obtained in-lens secondary electron (SE) and back scattered electron (BSE) signals of the 32 nm sputter coated Ca-alginate aerogel sample. The two images are identical, displayed in different color planes: (a) black/white and (b) red/white. The lighter colored spherical and cylindrical Au nanoparticles are well visible at the tips of the original Ca-alginate fibers in the images.

2. The hydration of the monolithic polyamide aerogel causes non-linear changes in its compressive strength. The hydration mechanism of polyamide aerogel was deduced, which provides an explanation for this phenomenon.

2.1) The 3D framework of polyamide aerogel consists of entangled and interconnected fibers. The thickness and length of the primary fibers vary greatly on the scale of a few tens of nanometers. Some of these threads are branched, and in some places, they run together in focal points.

2.2) The nitrogen-sorption isotherms of the polyamide aerogel belong to IUPAC category IV and are characterized by the H3 type hysteresis loop. The shape of the isotherms and the presence of a hysteresis loop are characteristic of mesoporous materials that also contain micropores to a significant extent. Macropores, that cannot be completely filled with condensed nitrogen, are also present, which can also be observed in the SEM images (Table 1).

Table 1. Structural parameters of polyamide aerogel estimated by the BET and the BJH methods from the N₂ adsorption-desorption data.

Parameter	Polyamide aerogel	Data evaluation
C-constant	59 ± 3	BET
Specific surface area (m²/g)	251 ± 20	BET
Total mesopore volume (cm³/g)	0.7 ± 0.1	BJH

2.3) Compared to the dry aerogel, the Young's modulus and the compressive strength increase dramatically with the increase of the water content of the aerogel, and show a maximum after conditioning at 50% relative humidity, i.e. a water content of 0.16 g/g (Figure 3). Interestingly, further hydration of the aerogel causes a steep decrease in these mechanical parameters.

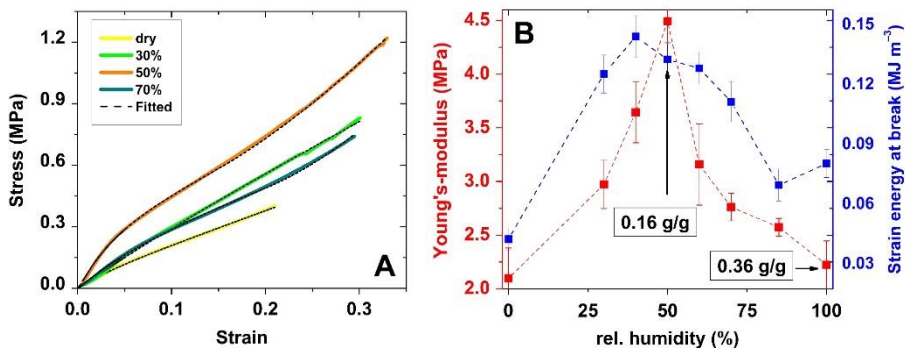


Figure 3. Results of monolithic polyamide aerogel compression tests. Panel A: Representative strain-stress curves of the dry and the partially hydrated aerogel monoliths. Panel B: The estimated Young’s modulus and compressive strength of the monolithic polyamide aerogel as a function of its conditioning in humid air.

In order to explain this phenomenon, the hydration mechanism of polyamide aerogel was studied using several methods. The processes at the molecular level were investigated with various NMR methods, and the changes in the nanostructure were followed by SANS.

2.4) The SANS results confirm the change in the morphology of the polyamide aerogel as a function of the water content. An increase in R_g indicates an increase in the size of the pores, which is accompanied by a smoothing of the surface of the pore walls, which is shown by the value $p \approx 4$ measured at 0.2 g/g water. Above this water content, the pore size still increases, although the roughness of the pore walls also increases. According to the SANS data, marked structural changes take place in the polyamide aerogel at the critical 0.2 g/g water content, and later when reaching 2.0 g/g water content (Figure 4).

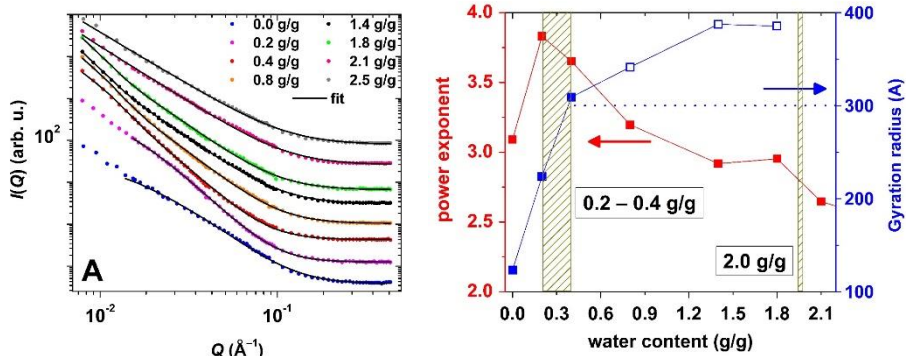


Figure 4. Small angle neutron scattering characterization of partially hydrated polyamide aerogel. Panel A: The experimental SANS curves (markers) together with the best fits (lines). Panel B: Estimated structural parameters as a function of the water content of polyamide aerogel. The estimated R_g values are uncertain above 300 \AA . The dashed vertical bars indicate water contents of special interest.

2.5) The high resolution of the ^{13}C CPMAS peaks measured by the solid-state NMR method suggests that the orientation of the polymer chains is somewhat ordered in the fibers after drying in supercritical CO_2 . The high intensity shoulder at 10 ppm in the ^1H MAS spectrum of the dry aerogel indicates the presence of multiple intermolecular H-bonds between the polymer molecules, which is typical for linear polyamides. The hydration of the aerogel does not change the ^{13}C chemical shifts in terms of peak widths and resolution but causes significant changes in relative peak intensities, which stabilize around 0.5 g/g water content. In accordance with this, the ^1H MAS spectrum of the partially hydrated samples shows that the extensive intermolecular H-bonding network of the linear polyamide molecules gradually breaks up with increasing hydration of the aerogel.

2.6) During the NMR relaxometric measurements, we observed 3 relaxation domains for the hydrated polyamide aerogel (Figure 5).

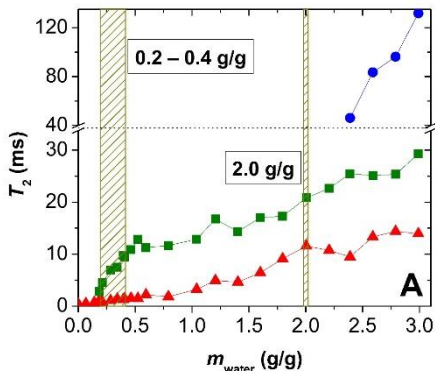


Figure 5. Results of the NMR relaxometry study of partially hydrated polyamide aerogel. The panels show the values of the transversal relaxation times (T_2) as the function of the water content. The dashed vertical bars indicate water contents of special interest.

At the lowest water contents, only one relaxation domain can be detected with very small T_2 values. This domain corresponds to those water molecules that interact strongly with polyamide macromolecules in H-bonding. The 2nd relaxation domain appears at a water content of about 0.19 g/g, with significantly higher T_2 values. However, these T_2 values are not high enough to indicate the formation of well-defined water droplets in the pores. Accordingly, the 2nd relaxation domain corresponds to water molecules still in strong interaction with the polyamide framework. The 3rd relaxation domain corresponds to the formation of well-defined water droplets and puddles in the focal points of the aerogel frame.

2.7) During the NMR diffusometry measurements, we changed two conditions: the water content of the polyamide aerogel and the observation time of the experiments. We have shown that two diffusion domains always appear at higher water content. The D_{obs} values of both ranges gradually increase with increasing the aerogel water content but only to a small extent. In addition, we found that the D_{obs} values do not change by changing the observation time of the NMR experiment, regardless of the water content.

2.8) We proved that in the case of partially hydrated polyamide aerogel, a ^1H NMR signal can only be measured starting from a water content of 1.0 g/g during the cryoporometry experiments. The cryoporometry results show that the pores of the hydrated polyamide aerogel are only partially filled with water droplets at a water content of 2.5 g/g. These droplets are first separated and enclosed by the hydrated polyamide nanofibers. However, these droplets coalesce and fill the available gap-like voids at a water content of 3.4 g/g without significantly changing the structure of the hydrated framework. The well-expressed decrease in the freezing point measured during the saturation of the pores shows that the solid framework remains well defined even in the case of complete hydration, i.e. the linear polymer molecules are still connected, no hydrogel is formed. This is consistent with the observations discussed for relaxometry and SANS.

2.9) Based on the summarized results of the NMR and SANS measurements, we identified the main steps of polyamide aerogel hydration, which are graphically summarized in Figure 6. The first water molecules bind to the surface of the polyamide nanofibers and fill the empty spaces in the intermolecular H-bonding network of the polyamide

macromolecules. These water molecules strengthen the H-bonding network that stabilizes the fibers, which causes the rearrangement of the nanostructure of the aerogel, which is clearly shown by the SANS results. In the state between 0.2 g/g and 0.4 g/g water content, the water molecules enter the entire volume of the polyamide nanofibers, integrate between the macromolecules and break some intermolecular H-bond sites. This weakens the strong intermolecular bonds characteristic of dry aerogel. Further hydration causes partial dissolution of the nanofibers, further increasing the pore size. This is accompanied by an increasing surface roughness of the partially dissolved polyamide fibers, as shown by the SANS results.

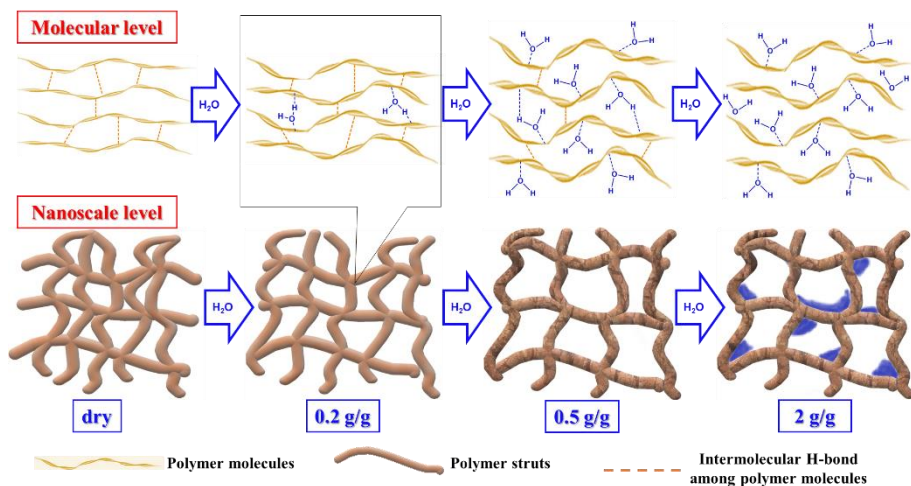


Figure 6. Graphical representation of the different stages of the hydration of the polyamide aerogel.

3. We have described in details the hydration mechanism of a polyimide aerogel.

3.1) A fibrous structure can also be observed in the case of the polyimide aerogel, however, in the case of polyimide, these fibers are much more uniform in size, less branched, and more separated. Due to the crosslinking agent that builds up the polyimide, the polymer itself has a 3D crosslinked chemical structure, which builds up the well-defined fibers.

3.2) We found that the nitrogen sorption isotherms of the polyimide aerogel are typical for mesoporous materials being category IV, and are characterized by an H3 hysteresis loop, which indicates the presence of macropores, also seen in the SEM images (Table 2).

Table 1. Structural parameters of polyimide aerogel estimated by the BET and the BJH methods from the N₂ adsorption-desorption data.

Parameter	Polyimide aerogel	Data evaluation
C-constant	55 ± 2	BET
Specific surface area (m ² /g)	297 ± 28	BET
Total mesopore volume (cm ³ /g)	0,8 ± 0,1	BJH

3.3) The chemical shifts in the solid-state NMR ¹³C CPMAS and ¹H MAS spectra do not change with the hydration of the aerogel. At the same time, the peak widths and the resolution also remain unchanged, only the dry sample differs slightly from the samples with different degrees of hydration. From this, we can conclude that the conformation of the

polyimide macromolecules does not change significantly as a result of hydration. The results do not indicate a strengthening segment movement either.

3.4) During the evaluation of the relaxometric measurements of the partially hydrated polyimide aerogel, we identified 3 relaxation domains (Figure 7).

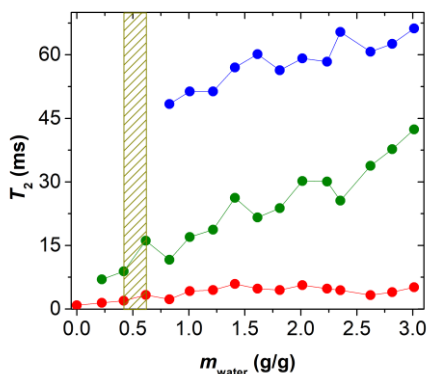


Figure 7. Results of the NMR relaxometry study of partially hydrated polyimide aerogel. The panels show the values of the transversal relaxation times (T_2) as the function of the water content. The dashed vertical bars indicate water contents of special interest.

At a very low water content, only one relaxation domain can be measured, which is bound to the polymer molecules by a strong secondary bond, so it can be assigned to water molecules with little mobility. The 2nd relaxation domain can already be detected at a water content of 0.2 g/g. This is typical of the water located inside the polyimide nanofibers and partially dissolving them. The 3rd relaxation domain also appears quickly, already at a water content of 0.8 g/g, which

shows high T_2 values typical of smaller water drops and puddles and increases continuously with the water content. This means that, in the case of polyimide aerogel, larger water layers and droplets appear on the surface of the fibers or between them, even at a low water content.

3.5) The self-diffusion of water cannot be measured in this system with at very low water contents. We first get a measurable signal at a water content of 0.8 g/g, which coincides with the appearance of the 3rd relaxation domain. In this system, therefore, diffusometry and relaxometry are consistent with each other.

3.6) We have proven that the droplet sizes calculated from the freezing curves in cryoporometry show a good agreement with the pore size distribution calculated from the nitrogen sorption measurements on dry aerogel for all tested water contents. In the case of samples with a water content of 2.0 g/g, we can determine based on the shape of the melting-freezing curves that the water is typically present in the form of spherical drops, and at a water content of 3.5 g/g, cylindrical water layers become more characteristic.

3.7) Considering the results of different characterization methods (NMR, SANS), we developed the hydration mechanism of the polyimide aerogel (Fig. 8).

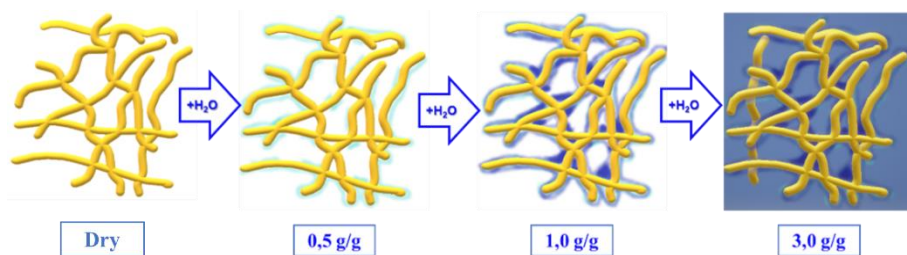


Figure 8. Graphical representation of the different stages of the hydration of the polyimide aerogel.

In the first step of polyimide aerogel hydration, the added small amount of water is able to form strong secondary bonds with the macromolecules and integrate into the nanofibers formed by them, which is evidenced by the existence of the 1st and 2nd relaxation domains and the corresponding small T_2 values. Then, adding additional water, the 3rd domain that appears at a water content of about 0.8 g/g can be associated with the water present on the surface of the fibers and between them. However, the original 3D structure of the polyimide macromolecules that build up the aerogel and the morphology of the framework changes only slightly when hydrated, as shown by SANS.

4. We proved that polyamide and polyimide aerogels are suitable for binding different drugs from supercritical carbon dioxide.

4.1) We successfully impregnated polyamide and polyimide aerogels with ibuprofen and ketoprofen in supercritical carbon dioxide under static conditions. We have developed the optimal conditions for the impregnation of polymer aerogels. We determined the total amount of active ingredient bound by the aerogels in methanol using the UV-vis photometric method. (Table 3).

Table 3. The total amount of drugs in polymer aerogels.

Aerogels	Ibuprofen [w/w %]	Ketoprofen [w/w %]
Polyamide aerogel	25,3 ± 1,31	3,45 ± 0,17
Polyimide aerogel	15,9 ± 0,85	7,97 ± 0,68

4.2) The structure of the impregnated drugs was investigated using X-ray diffraction spectrometry, and it was established that they are found in an amorphous form in the mesoporous carriers. Thus, we proved the use of aerogels as pharmaceutical technology solubilizing agents.

5. We proved that aerogels impregnated with drugs release the drugs in different ways depending on the pH of the release media. By analyzing the dissolution profiles and considering the hydration mechanism of the aerogels, we proposed the mechanisms of drug release from polymer aerogels.

5.1) In the case of the release of the ketoprofen in a hydrochloric acid, we found that the hydrophobic interaction between the polymer carriers and the drug is the controlling factor, which is evidenced by the very small dissolution percentage (Table 4).

Table 4. The maximum amount of ketoprofen released from the aerogels is given as a percentage compared to the impregnated amount.

Ketoprofen	HCl (pH=1)	PBS (pH=7,4)
Polyamide aerogel	23 %	30 %
Polyimide aerogel	5 %	25 %

It is likely that a real sorption equilibrium develops between the drug and the aerogel framework. In addition, the poor solubility of the drug also contributes to the small amount of dissolved drug in both polymer aerogels. Based on the zeta-potential values in PBS release medium, at a pH=7.0, polyamide has most probably a positive surface charge, polyimide has most probably a negative surface charge, and ketoprofen is present in deprotonated form, i.e. as an anion. Although the solubility of ketoprofen increases because of this, the rate of dissolution is ultimately reduced even at this pH, probably due to the strong interaction with the polymers.

5.2) During the study of the release of the ibuprofen in hydrochloric acid, we found that the solubility of ibuprofen is relatively low in hydrochloric acid. A very small difference can be observed in the drug release of the two aerogels (Table 5).

Table 5. The maximum amount of ibuprofen released from the aerogels is given as a percentage compared to the impregnated amount.

Ibuprofen	HCl (pH=1)	PBS (pH=7,4)
Polyamide aerogel	38 %	90 %
Polyimide aerogel	47 %	80 %

The hydrophobic interaction is also significant here. The solubility of ibuprofen in PBS is much better than in acidic media. Both the polyimide aerogel and the drug have negative charge, which on the one hand promotes their hydration, and on the other hand, the Coulomb interaction greatly favors the release, so the active ingredient dissolves instantly. This case is most favorable for the use of aerogels as solubilizing agents.

Hydration mechanisms and drug delivery applications of polymer aerogels

In the case of polyamide aerogel, the reason for the restraining effect is the Coulomb interaction between the positive surface charge of the aerogel and the deprotonated drug.

IV. Possible utilization of the results

During our research, we studied the preparation and the characterization of synthetic polymer-based aerogels, a group of a very promising material family. We performed a detailed study of two of their representatives, a polyamide and a polyimide aerogel. Using several methods, we investigated the changes in the structure of the aerogel framework due to interaction with water (moisture); and based on the results, we proposed a hydration mechanism for both aerogels. Furthermore, we investigated the use of these aerogels as solubilizing agents in pharmaceutical technology.

If aerogels are designed for use in moist air or aqueous media, such as for biomedical or engineering applications, it is essential to understand the mechanism of hydration of the aerogel framework and the resulting modification of the aerogel structure. The investigation of these properties contributes to the exploration of additional application areas.

Articles related to the dissertation

Foreign language scientific articles in international journals

1. K. Moldován; A. Forgács; G. Paul; L. Marchese; A. Len; Z. Dudás; S. Kéki; I. Fábíán; J. Kalmár:
Mechanism of Hydration Induced Stiffening and Subsequent Plasticization of Polyamide Aerogel
ADVANCED MATERIALS INTERFACES 2300109 (2023)
IF (2022): 5,4 (D1)
2. L. Juhász; K. Moldován; P. Gurikov; F. Liebner; I. Fábíán; J. Kalmár; Cs. Cserháti
False Morphology of Aerogels Caused by Gold Coating for SEM Imaging
POLYMERS, 13(4), 588. (2021)
IF (2021): 4,967 (Q1)

Articles not detailed in the dissertation

1. P. Herman; K. Moldován; G. Paul; L. Marchese; Z. Balogh; A. Len; Z. Dudás; I. Fábíán; J. Kalmár:
Selective and Reversible Surface Complexation of Aqueous Palladium(II) by Polycarboxylate (Pyromellitic Acid) Functionalized Hybrid Aerogel Sorbent
APPLIED SURFACE SCIENCE 613 Paper: 156026, 14 p. (2022)
IF (2021): 6,7 (Q1)
2. N. Lihi; Z. Balogh; R. Diószegi; A. Forgács; K. Moldován; N. V. May; P. Herman; I. Fábíán; J. Kalmár:
Functionalizing Aerogels with Tetraazamacrocyclic Copper(II) Complexes: Nanoenzymes with Superoxide Dismutase Activity
APPLIED SURFACE SCIENCE 611: Part A Paper: 155622, 12 p. (2022)
IF (2021): 6,7 (Q1)

3. L. Juhász; K. Moldován; P. Herman; Z. Erdélyi; I. Fábíán; J. Kalmár;
Cs. Cserhádi:
Synthesis and Stabilization of Support-Free Mesoporous Gold Nanoparticles
NANOMATERIALS 10: 6 Paper: 1107, 11 p. (2020)
IF (2020): 5,076 (Q1)

4. I. Lázár; A. Forgács; A. Horváth; G. Király; G. Nagy; A. Len; Z. Dudás; V. Papp; Z. Balogh; K. Moldován; L. Juhász; Cs. Csaba; Zs. Szántó; I. Fábíán; J. Kalmár:
Mechanism of Hydration of Biocompatible Silica-Casein Aerogels Probed by NMR and SANS Reveal Backbone Rigidity
APPLIED SURFACE SCIENCE 531 Paper: 147232, 13 p. (2020)
IF (2020): 6,707 (D1)

5. A. Forgács; K. Moldován; P. Herman; E. Baranyai; I. Fábíán; G. Lente; J. Kalmár:
Kinetic Model for Hydrolytic Nucleation and Growth of TiO₂ Nanoparticles.
JOURNAL OF PHYSICAL CHEMISTRY C 122 (33), 19161-19170 (2018)
IF (2018): 4,309 (D1)

Oral and poster presentations

1. O-E. Odongerel, A. Ademi, K. Moldován, J. Kalmár
Synthesis and Characterization of Flexible Polyimide Aerogels
Workshop on Aerogels Characterization and Modelling
2023. 03. 29-31., Debrecen, Magyarország
2. K. Moldován, A. Forgács, J. Kalmár
Effect of water content on the mechanical properties of high molecular weight polyamide aerogel
2nd International Conference on Aerogel for Biomedical and Environmental Applications
2022. 06. 28. – 07. 02., Athén, Görögország
3. K. Moldován, A. Forgács, J. Kalmár
Effect of water sorption on the structures of polyimide and polyamide aerogels
Athens Conference on Advances in Chemistry
2022. 06. 28. – 07. 02., Athén, Görögország
4. L. Juhász, K. Moldován, P. Gurikov, F. Liebner, I. Fábíán, J. Kalmár, C. Cserhádi
False Morphology of Aerogels Caused by Gold Coating for SEM Imaging
Athens Conference on Advances in Chemistry
2021. 03. 10-14., Athén, Görögország
5. K. Moldován, A. Forgács, A. Len, Z. Dudás, I. Fábíán, J. Kalmár
Hydration Mechanism of Polyimide and Polyamide Aerogels Investigated by NMR Spectroscopy and SANS Techniques
5th International Seminar on Aerogel
2020. 09. 16-18., Hamburg, Németország

BSc and MSc thesis

1. Odongerel Oyun-Erdene: **Synthesis and characterization of polyimide aerogels** (MSc, 2023.)
Supervisors: Dr. Kalmár József, Moldován Krisztián Eduárd
2. Pálócziné Győrfi Szilvia: **Gyógynövény hatóanyagok extrahálása és impregnálása aerogélekre** (MSc, 2021.)
Supervisors: Dr. Kalmár József, Moldován Krisztián Eduárd
3. Bazsó László: **Polimer alapú aerogélek mint gyógyszer-hatóanyagok hordozói** (MSc, 2021.)
Supervisors: Dr. Kalmár József, Moldován Krisztián Eduárd
4. Pércsi Dániel: **Polimer aerogélek előállítása és falhasználása gázseparációra** (MSc, 2021.)
Supervisors: Dr. Kalmár József, Moldován Krisztián Eduárd
5. Török Andor: **Gyógyszerhatóanyagok kioldódása impregnált polimer aerogélekből** (BSc, 2021.)
Supervisors: Dr. Kalmár József, Moldován Krisztián Eduárd
6. Pércsi Dániel: **Poliamid alapvázú aerogélek előállítása és tulajdonságai** (BSc, 2019.)
Supervisors: Dr. Kalmár József, Moldován Krisztián Eduárd



Registry number: DEENK/370/2023.PL
Subject: PhD Publication List

Candidate: Krisztián Moldován
Doctoral School: Doctoral School of Chemistry
MTMT ID: 10070099

List of publications related to the dissertation

Foreign language scientific articles in international journals (2)

1. **Moldován, K.**, Forgács, A., Paul, G., Marchese, L., Len, A., Dudás, Z., Kéki, S., Fábíán, I., Kalmár, J.: Mechanism of Hydration Induced Stiffening and Subsequent Plasticization of Polyamide Aerogel.
Adv Materials Inter. 10 (17), 1-15, 2023. ISSN: 2196-7350.
DOI: <http://dx.doi.org/10.1002/admi.202300109>
IF: 5.4 (2022)
2. Juhász, L., **Moldován, K.**, Gurikov, P., Liebner, F., Fábíán, I., Kalmár, J., Cserháti, C.: False Morphology of Aerogels Caused by Gold Coating for SEM Imaging.
Polymers. 13 (4), 1-12, 2021. EISSN: 2073-4360.
DOI: <http://dx.doi.org/10.3390/polym13040588>
IF: 4.967

List of other publications

Foreign language scientific articles in international journals (5)

3. Lihi, N., Balogh, Z., Diószegi, R., Forgács, A., **Moldován, K.**, May, N. V., Herman, P., Fábíán, I., Kalmár, J.: Functionalizing Aerogels with Tetraazamacrocyclic Copper(II) Complexes: Nanoenzymes with Superoxide Dismutase Activity.
Appl. Surf. Sci. 611, 1-12, 2022. ISSN: 0169-4332.
DOI: <http://dx.doi.org/10.1016/j.apsusc.2022.155622>
IF: 6.7
4. Herman, P., **Moldován, K.**, Paul, G., Marchese, L., Balogh, Z., Len, A., Dudás, Z., Fábíán, I., Kalmár, J.: Selective and reversible surface complexation of aqueous palladium(II) by polycarboxylate (pyromellitic acid) functionalized hybrid aerogel sorbent.
Appl. Surf. Sci. 613, 1-14, 2022. ISSN: 0169-4332.
DOI: <http://dx.doi.org/10.1016/j.apsusc.2022.156026>
IF: 6.7





5. Lázár, I., Forgács, A., Horváth, A., Király, G., Szemán-Nagy, G., Len, A., Dudás, Z., Papp, V., Balogh, Z., **Moldován, K.**, Juhász, L., Cserhádi, C., Szántó, Z., Fábíán, I., Kalmár, J.: Mechanism of hydration of biocompatible silica-casein aerogels probed by NMR and SANS reveal backbone rigidity.
Appl. Surf. Sci. 531, 1-13, 2020. ISSN: 0169-4332.
DOI: <http://dx.doi.org/10.1016/j.apsusc.2020.147232>
IF: 6.707
6. Juhász, L., **Moldován, K.**, Herman, P., Erdélyi, Z., Fábíán, I., Kalmár, J., Cserhádi, C.: Synthesis and Stabilization of Support-Free Mesoporous Gold Nanoparticles.
Nanomaterials. 10 (6), 1-11, 2020. EISSN: 2079-4991.
DOI: <http://dx.doi.org/10.3390/nano10061107>
IF: 5.076
7. Forgács, A., **Moldován, K.**, Herman, P., Baranyai, E., Fábíán, I., Lente, G., Kalmár, J.: Kinetic Model for Hydrolytic Nucleation and Growth of TiO₂ Nanoparticles.
J. Phys. Chem. C. 122 (33), 19161-19170, 2018. ISSN: 1932-7447.
DOI: <http://dx.doi.org/10.1021/acs.jpcc.8b04227>
IF: 4.309

Total IF of journals (all publications): 39,859

Total IF of journals (publications related to the dissertation): 10,367

The Candidate's publication data submitted to the iDEa Tudóstér have been validated by DEENK on the basis of the Journal Citation Report (Impact Factor) database.

16 August, 2023

